DOI:
10.1109/ISBI.2018.8363772

Document Version
Peer reviewed version

FULLY AUTOMATED MYOCARDIAL STRAIN ESTIMATION FROM CINE MRI USING CONVOLUTIONAL NEURAL NETWORKS

Esther Puyol-Antón[1], *Bram Ruijsink*[1,3], *Wenjia Bai*[4], *Hélène Langet*[2], *Mathieu De Craene*[2], *Julia A. Schnabel*[1] *Paolo Piro*[2], *Andrew P. King*[1*], *Matthew Sinclair* [4*]

[1]School of Biomedical Engineering & Imaging Sciences , King's College London, UK
[2] Philips Research, Medisys, Paris, France
[3] Guy's and St Thomas' Hospital NHS Foundation Trust, London, UK
[4] Biomedical Image Analysis Group, Department of Computing, Imperial College London, UK

ABSTRACT

Cardiovascular magnetic resonance myocardial feature tracking (CMR-FT) is a promising method for quantification of cardiac function from standard steady-state free precession (SSFP) images. However, currently available techniques require operator dependent and time-consuming manual intervention, limiting reproducibility and clinical use. In this paper, we propose a fully automated pipeline to compute left ventricular (LV) longitudinal and radial strain from 2- and 4-chamber cine acquisitions, and LV circumferential and radial strain from the short-axis imaging. The method employs a convolutional neural network to automatically segment the myocardium, followed by feature tracking and strain estimation. Experiments are performed using 40 healthy volunteers and 40 ischemic patients from the UK Biobank dataset. Results show that our method obtained strain values that were in excellent agreement with the commercially available clinical CMR-FT software CVI_{42} (Circle Cardiovascular Imaging, Calgary, Canada).

Index Terms— Myocardial Strain, Automatic pipeline, Machine learning, MRI

1. INTRODUCTION

Myocardial wall motion analysis (MWMA) allows for precise and comprehensive assessment of left ventricular (LV) and right ventricular (RV) contractile function. Myocardial strain and strain rate provide a relatively load-independent quantitative evaluation of myocardial wall motion, and have been shown to enable earlier and more sensitive detection of myocardial diseases compared to global measures of cardiac function, such as ventricular volumes and ejection fraction [1]. In echocardiography, strain can be measured by tracking naturally occurring acoustic markers ('speckles') in the myocardium throughout the cardiac cycle. However, the limited acquisition windows severely restrict the ability to interrogate total myocardial wall motion. Cardiac magnetic resonance (CMR) is the current gold standard for assessment of global and regional myocardial function, and does not suffer from limited acquisition windows. Several CMR imaging techniques have been proposed for strain analysis, such as myocardial tagging, phase contrast velocity imaging, displacement encoding, and strain encoding. Although all of these CMR techniques provide useful information on myocardial function, they are not typically used in routine clinical CMR as they require additional imaging and complex, time-consuming post-processing. Instead, CMR feature tracking (CMR-FT) has been proposed as a more accessible MWMA technique. By tracking features between consecutive frames from steady state free precession (SSFP) cine acquisitions, in a way analogous to speckle tracking echocardiography, CMR-FT is able to derive strain and strain rate from routinely acquired CMR images. However, current CMR-FT techniques typically require manual delineation of cardiac volumes and frequent reassessment of annotations based on tracking results, which is skill and experience dependent. This results in increased processing times and a significant degree of inter and intra-observer variability [2].

Related Work: The two most common commercially available software packages offering CMR-FT are TomTec (TomTec Imaging Systems, Unterschleissheim, Germany) and CVI_{42} (Circle Cardiovascular Imaging, Calgary, Canada). Both require manual segmentation of the end-diastolic (ED) frame and identification of mitral valve insertion points. Some semi-automatic methods have been proposed, for example Mansi *et al.,* [3] presented an improvement of the diffeomorphic Demons algorithm for cine MR sequences. They compared the estimated strain using the proposed motion tracking algorithm to tagged-MR estimated strains for a healthy volunteer,

This work is funded by the Kings College London & Imperial College London EPSRC Centre for Doctoral Training in Medical Imaging (EP/L015226/1) and supported by the Wellcome EPSRC Centre for Medical Engineering at Kings College London (WT 203148/Z/16/Z). This research has been conducted using the UK Biobank Resource under Application Number 17806.

* Joint last authors.

and with ultrasound 2-D strain for a patient with congenital pulmonary valve regurgitations. However, their method required manual input for segmentation and motion correction. Few automatic pipelines have been proposed before and most either focus on one type of strain, or on a single slice. For example, Jolly *et al.,* [4] proposed an automatic pipeline to measure LV mean mid-wall Eulerian circumferential strain from cine SSFP. More recently, Vigneault *et al.,* [5] proposed an automatic pipeline for estimation of circumferential cardiac strain using deep learning, although did not make a direct comparison to any clinical software.

Contributions: In this paper we propose a fully automatic pipeline to quantify myocardial longitudinal, radial and circumferential strain from cine MR sequences. The pipeline enables fast and accurate assessment of LV strains and eliminates manual intervention and inter and intra-observer variation. To validate the proposed method we compared the obtained strain values with those computed using CVI_{42}, a widely used clinical tissue-tracking CMR software package.

2. MATERIAL

The study population consisted of 40 healthy volunteers and 40 ischemic patients from the UK Biobank Imaging Study [6], with demographics displayed in Table 1. CMR imaging was carried out on a 1.5 Tesla scanner (Siemens Healthcare, Erlangen, Germany). Short-axis (SA) stacks covering the full heart, and two orthogonal long-axis (LA) planes (2-chamber (2Ch) and 4-chamber (4Ch) views) were available for each subject (TR/TE = $2.6/1.10$ ms, flip angle = $80°$). In-plane resolution of the SA stack and LA images was 1.8 mm, with slice thickness of 8 mm and 6 mm for SA and LA respectively. 50 frames were acquired per cardiac cycle.

Table 1: Study demographics: end-diastolic volume (EDV); end-systolic volume (ESV); ejection fraction (EF), all expressed as mean (standard deviation); and age expressed as mean (min-max).

Demographics	**Healthy volunteers**	**Ischemic patients**
Study population, n	40	40
Age (years)	60.20 (43-73)	66.75 (51-73)
LV-EDV (mL/m^2)	141.43 (33.74)	175.47 (48.82)
LV-ESV (mL/m^2)	55.61 (15.67)	84.28 (35.72)
LV-EF (%)	60.85 (4.78)	55.08 (7.93)

3. METHODS

The proposed framework for automatically quantifying myocardial strain from cine MR sequences is summarized in Fig. 1, and each step is described below.

Automatic Segmentation Network: A fully-convolutional network (FCN) with a 17 convolutional layer VGG-like architecture was used for the automatic segmentation of the LV myocardium and blood-pool at ED for SA and LA slices[7, 8].

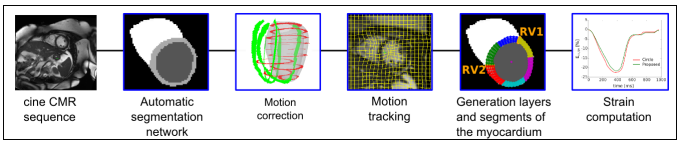

Fig. 1: Overview of the proposed framework for automatic quantification of myocardial strain from cine MR sequence.

Each convolutional layer of the network is followed by batch normalisation and ReLU, except the last one, which is followed by the softmax function. In the case of the SA stack, each slice is segmented independently, i.e. in 2D. From the segmentations, a bounding box was generated and used to crop the image to only include the desired FoV, improving pipeline speed and reducing errors in motion tracking.

Motion correction: Automatic SA and LA segmentations were used to correct breath-hold induced motion artefacts using the iterative registration algorithm proposed in [7]. The motion-corrected LA/SA slices are used to correctly identify mid-cavity SA planes for computing strain, determined by correspondence to the valves and apex identified in the LA view.

Motion tracking: Motion tracking was performed on each 2D plane in both SA and LA views using MIRTK[1]; more specifically, a 2D B-spline free-form deformation (FFD) registration was used [9] to estimate LV motion between consecutive frames of the cine MR sequences.

Generation of layers and segments of the myocardium. On the ED frame, the LV myocardium was divided into 5 layers and 6 segments as illustrated in Fig. 2, and described below. From the SA and LA segmentations, the contours defining the boundaries of the LV endocardium and epicardium were extracted using standard morphological operations. Both contours were smoothed by fitting a spline with the same number of equally-spaced points for both. Skeletonization was used to generate a centreline of the myocardial segmentation in both the SA and LA views. Centrelines were smoothed by fitting a further spline. Two additional contours were generated at the midline of the centreline-epicardium and centreline-endocardium. In addition, the RV-LV intersection were automatically detected (RV1 and RV2 in Fig. 2) and used to divide the 5 concentric trans-mural contours within the LV were into six sectors (2 segments in the septum and 4 segments on the free wall) along the arc-length of the myocardial centreline for the SA views. Similarly, the LA view was divided into six equal-sized sectors (see Fig. 2). Finally, all spline points were transformed with the motion tracking deformation fields.

Strain computation: Myocardial strain defines the total deformation of a region of tissue during the cardiac cycle relative to its initial configuration at the onset of the cardiac cycle, and it is normally expressed in percentages. Three

[1] http://www.biomedia.doc.ic.ac.uk/software/mirtk/

components of myocardial strain (radial, rr, circumferential, cc, and longitudinal, ll) are typically measured, and each component used to quantify different aspects of cardiac function. More specifically, the mean Lagrangian strain over the whole myocardium for each strain component j (i.e. rr, cc or ll) at each time point t was computed as follows:

$$E^t_{j,v} = \sum_{s=1}^{S}\sum_{k=1}^{K} \frac{1}{SK} \frac{d^t_{j,v,k,s} - d^{ED}_{j,v,k,s}}{d^{ED}_{j,v,k,s}} \quad (1)$$

where $d^{ED}_{j,v,k,s}$ is the length at ED for the segment s, layer k and view v (i.e. SA or LA) for strain component j. Radial strain was computed with transmural distance (d_r in Fig. 2) from SA/LA slices; circumferential strain using circumferential segment arclength (d_c in Fig. 2) from SA slices; and longitudinal strain using longitudinal segment arclength from LA slices. Because there are five layers, we can calculate the endocardial, epicardial, midwall, endo-midwall and epi-midwall strain separately. Global strain was computed as the average of the estimated strains from each segment and layer to reduce noise.

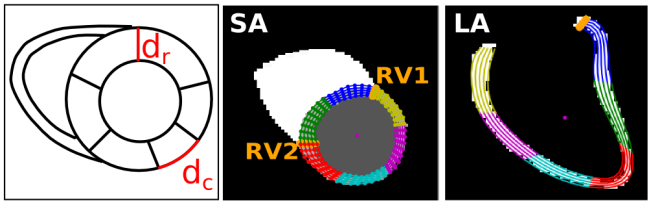

Fig. 2: **Left**: Schema of the SA segments with radial distance d_r and circumferential distance d_c. **Middle**: SA segmentation with 5 concentric contours within the LV wall and six sectors. **Right:** LA segmentation split into 5 layers and 6 segments. Colours represent segments.

4. RESULTS

The strain values obtained using the proposed automatic method were compared with strain analysis obtained by a level 2 cardiologist using CVI_{42}. Importantly, the manual segmentations created in CVI_{42} were made independently of the proposed automated framework and strain results were computed as the mean of three analysis repetitions, according to clinical consensus [2]. Furthermore, the segmentation deep learning network was trained and optimised using a different data set. The 2Ch and 4Ch LA slices were used to determine LV longitudinal strain and LV radial strain ($E^t_{ll,LA}$ and $E^t_{rr,LA}$) alongside the time to peak (TPK) strain duration. LV SA circumferential ($E^t_{cc,SA}$) and radial ($E^t_{rr,SA}$) strains and the corresponding TPK strain durations were calculated from three mid-ventricular SA slices determined automatically in the proposed approach. The same slices were also used in CVI_{42}. Peak LV strain values obtained using the proposed method and CVI_{42} were compared using a Welch's $t-$test (significant differences reported for p-value$<$ 0.05 with Bonferroni's correction). Moreover, peak LV strain values between healthy volunteers and ischemic patients were compared using a $t-$test (significant differences reported for p-value$<$ 0.05 with Bonferroni's correction) for the proposed method and CVI_{42}. Fig. 3 shows an example of the three strains estimated for a healthy volunteer and an ischemic patient. Experiments were carried out on a PC with a Intel Xeon CPU E5-1660 v3 with 31GiB RAM, and the running time of the proposed pipeline for each subject is 200s.

Quantification of LV strain. Table 2 shows the average peak strain values of 40 healthy volunteers and 40 ischemic patients using both methods. Our results show there is no statistical difference between the two methods for peak $E_{rr,LA}$ and $E_{rr,SA}$ in both patients and volunteers. Only in healthy volunteers, $E_{ll,LA}$ and $E_{cc,SA}$ were slightly underestimated with the proposed method compared to CVI_{42}. Furthermore, the proposed method was successful in detecting statistically significant decreased peak strain in ischemic patients compared to healthy volunteers, similarly to CVI_{42}.

Table 2: Comparison of strain results derived from CVI_{42} and the proposed pipeline for the cohort, reported as mean (SD). Asterisks indicate significant differences between proposed methid and CVI_{42}. Daggers indicate statistically significant differences between healthy volunteers and ischemic patients.

	Healthy volunteers	
	CVI_{42}	**Proposed**
Peak $E_{ll,LA}$(%)	-20.26 (2.44)	-18.17 (2.49)*
TPK $E_{ll,LA}$(ms)	343.75 (44.41)	383.68 (53.83)
Peak $E_{rr,LA}$(%)	37.11 (7.52)	36.70 (7.97)
TPK $E_{rr,LA}$(ms)	343.75 (44.41)	387.33 (52.24)
Peak $E_{rr,SA}$(%)	43.07 (7.10)	42.31 (8.48)
TPK $E_{rr,SA}$(ms)	336.25 (36.04)	337.93 (33.97)
Peak $E_{cc,SA}$(%)	-22.02 (2.11)	-19.94 (2.56)*
TPK $E_{cc,SA}$(ms)	330.60 (40.63)	331.58 (46.92)
	Ischemic patients	
	CVI_{42}	**Proposed**
Peak $E_{ll,LA}$(%)	-17.19 (4.26)†	-16.09 (4.29)†
TPK $E_{ll,LA}$(ms)	367.50 (66.02)	366.90 (62.53)
Peak $E_{rr,LA}$(%)	29.67 (10.36)†	31.54 (10.33)†
TPK $E_{rr,LA}$(ms)	339.00 (58.74)	369.64 (64.72)
Peak $E_{rr,SA}$(%)	32.32 (8.99)†	31.70 (9.81)†
TPK $E_{rr,SA}$(ms)	355.27 (34.28)	349.73 (35.26)
Peak $E_{cc,SA}$(%)	-18.22 (3.40)†	-18.02 (3.78)†
TPK $E_{cc,SA}$(ms)	362.03 (45.56)	362.03 (61.84)

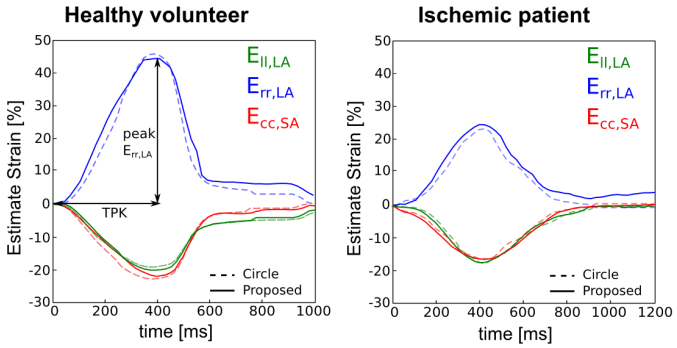

Fig. 3: Examples of estimated strains for a healthy volunteer and an ischemic patient. Figure shows global strain curves, peak strain and TPK.

Variability between CVI_{42} and proposed method. The variation in peak strain estimation between the two methods was assessed using Bland-Altman analysis and Intraclass correlation coefficients (ICC) (see Fig. 4). The level of agreement was defined as in [2]: excellent for ICC>0.74, good for ICC=0.6-0.74, fair for ICC=0.40-0.59, and poor for ICC<0.4. Results show excellent agreement between our method and CVI_{42}, with the lowest variation in peak $E_{ll,LA}$ and $E_{cc,SA}$, whereas a larger spread was observed for peak radial strain. The latter is in line with the larger intra and inter observer variability seen in radial strain assessment in previously published CMR-FT literature [1].

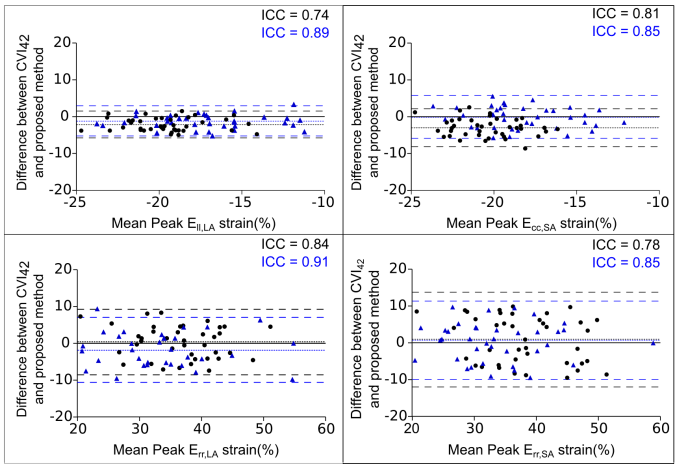

Fig. 4: Bland Altman plots between CVI_{42} and the proposed pipeline for peak global strain (%). Healthy volunteers are shown as black circles and ischemic patients as blue triangles. Dotted lines correspond to the mean difference between methods, and dashed lines correspond to the limits of agreement (95% confidence).

5. DISCUSSION AND CONCLUSIONS

Automatic quantification of cardiac function from cine CMR sequences has the potential to increase accessibility of MWMA for assessment of cardiac diseases by eliminating time consuming manual post-processing steps and reducing inter- and intra-observer variation. In this paper, we have presented a fully automated pipeline for LV strain estimation that includes segmentation, motion tracking and longitudinal, radial and circumferential strain estimation from routinely acquired CMR imaging. This is the first time that such a pipeline has been described. We compared the performance of the proposed method with CVI_{42}, one of the two commercially available software packages for CMR-FT. Our method showed excellent agreement with strain analysis manually obtained by an expert in CVI_{42}. The method slightly underestimated peak longitudinal and circumferential strain compared to CVI_{42}, most likely reflecting minor differences in motion tracking algorithms. However, this underestimation was consistent throughout the range of strains observed in our study. We also note that, although widely used clinically, tools such as CVI_{42} cannot be considered as gold standards for strain quantification due to their intra and inter observer variability. Future work will focus on extending the strain computation to a larger cohort and to multiple pathologies. Furthermore, our method allows for assessment of regional 2D strain and can be easily extended to 3D strain, which can be used in the future for more comprehensive regional MWMA.

6. REFERENCES

[1] P Claus et al., "Tissue tracking technology for assessing cardiac mechanics: principles, normal values, and clinical applications," *JACC: Cardiovascular Imaging*, vol. 8, no. 12, pp. 1444–1460, 2015.

[2] A Schuster et al., "Cardiovascular magnetic resonance feature-tracking assessment of myocardial mechanics: Intervendor agreement and considerations regarding reproducibility," *Clinical radiology*, vol. 70, no. 9, pp. 989–998, 2015.

[3] T Mansi et al., "Physically-constrained diffeomorphic demons for the estimation of 3d myocardium strain from cine-mri," *Functional Imag. Modeling Heart.*, pp. 201–210, 2009.

[4] M-P Jolly et al., "Automated assessments of circumferential strain from cine CMR correlate with LVEF declines in cancer patients early after receipt of cardiotoxic chemotherapy," *Journal of Cardiovascular Magnetic Resonance*, vol. 19, no. 1, pp. 59, 2017.

[5] DM Vigneault et al., "Feature tracking cardiac magnetic resonance via deep learning and spline optimization," *Functional Imag. Modeling Heart.*, p. 183, 2017.

[6] SE Petersen et al., "UK Biobanks cardiovascular magnetic resonance protocol," *Journal of cardiovascular magnetic resonance*, vol. 18, no. 1, pp. 8, 2016.

[7] M Sinclair et al., "Fully automated segmentation-based respiratory motion correction of multiplanar cardiac magnetic resonance images for large-scale datasets," in *Med. Image Comput. Comput. Assist. Interv (MICCAI)*. Springer, 2017, pp. 332–340.

[8] W Bai et al., "Semi-supervised learning for network-based cardiac MR image segmentation," in *Med. Image Comput. Comput. Assist. Interv (MICCAI)*, 2017, pp. 253–260.

[9] D Rueckert et al., "Nonrigid registration using free-form deformations: application to breast mr images," *IEEE Trans. Med. Imag.*, vol. 18, no. 8, pp. 712–721, 1999.